LUMBER DRYING STRESSES AND MITIGATION OF CROSS-SECTIONAL DEFORMATION

Zhouyang Xiang

Graduate Research Assistant
E-mail: zxiang@ncsu.edu

*Perry Peralta**†

Associate Professor
E-mail: perry_peralta@ncsu.edu

Ilona Peszlen†

Associate Professor
Department of Forest Biomaterials
North Carolina State University
Raleigh, NC 27695-8005
E-mail: ilona_peszlen@ncsu.edu

(Received August 2011)

Abstract. Lumber drying is a time-consuming and energy-intensive operation that is complicated by shrinkage, which occurs when wood moisture content falls below FSP. Differential shrinkage between radial and tangential directions results in cross-sectional strains that cost the wood industry a substantial amount of money. A novel approach that uses the concept of drying stresses has the potential to mitigate this problem. This study investigated the feasibility of applying an impervious coating to lumber surfaces to induce stresses that minimize a drying distortion called cupping. Flatsawn and quartersawn southern red oak (*Quercus falcata*) lumber samples from 10 trees were analyzed. Specimens from the same lumber were randomly assigned to three treatments: uncoated, pith-side coated, and bark-side coated for flatsawn specimens; and uncoated, upper-side coated, and bottom-side coated for quartersawn specimens. Quartersawn specimens showed very limited distortion for all three treatments. Cupping was minimized in pith-side-coated flatsawn specimens but exacerbated in bark-side-coated flatsawn specimens. Experimental strains for flatsawn uncoated specimens agreed with those predicted using a numerical model.

***Keywords*:** Southern red oak, *Quercus falcata*, shrinkage, cupping, drying stresses, modeling.

INTRODUCTION

Lumber drying is an important process prior to manufacturing all sorts of wood products. Drying improves wood's machinability, resistance to biodeterioration, adhesion with glues or finishes, treatability with chemicals, and transportation cost. However, lumber drying is time-consuming and energy-intensive, representing 7-15% of the lumber industry's energy requirement (Ferguson 1997). Drying also results in wood shrinkage. When wood moisture content falls below FSP, water molecules residing within the amorphous regions of the microfibrils start to evaporate, causing cell walls and the whole lumber piece to shrink. Because of shrinkage anisotropy and drying stresses, undesirable deformation and defects often accompany lumber drying. The wood industry loses a substantial amount of money each year because of drying defects. Cupping is one of those defects. Cupping happens because shrinkage parallel is greater than that perpendicular to the growth rings. In other words, cupping is the result of tangential shrinkage of wood being greater than radial shrinkage, and the greater the difference, the more severe the degree of

* Corresponding author
† SWST member

cupping. Current methods used to deal with wood cupping include using a moderate drying schedule and applying a restraining weight on lumber during drying (FPL 2001). Limited work has been done on developing new approaches to minimizing wood cupping. We hypothesize that cupping can be mitigated if unbalanced drying stresses are induced on opposite faces of flatsawn lumber. This can be easily implemented by a method that is described in this article. Also, the amount of cupping in lumber will be quantified by modifying an existing cross-sectional shrinkage distortion theory (Booker et al 1992; Booker 2003).

MATERIALS AND METHODS

Lumber

One piece of lumber was obtained from each of 10 southern red oak (*Quercus falcata*) trees. Five pieces were flatsawn, and five were quartersawn. Each piece was 6 m long and about 30 mm thick. Four flatsawn pieces were about 160 mm wide; the fifth was about 340 mm wide. Four quartersawn lumber were about 140 mm wide, and the fifth was 230 mm wide. All boards were 100% heartwood, except for flatsawn boards F2 and F3 (Table 1), which were 95 and 70% heartwood, respectively. All samples were soaked in water to keep them wet and prevent fungal decay.

One hundred twenty pieces of 254-mm-long specimens were prepared from the lumber. The transverse surfaces of each specimen were scanned to obtain images of growth ring orientation. When the lumber was being cut, a 25-mm-long moisture section was sawn off each end of the specimen. Moisture sections were weighed and then oven-dried to determine their moisture content and predict oven-dry mass of each specimen. Moisture content of specimens in the dry kiln can thus be estimated, and the drying process can be monitored.

Coating and Drying Schedule

Three adjacent flatsawn specimens were randomly assigned to three coating treatments: coating on the tangential surface close to the bark (bark-side-coated), coating on the tangential surface close to the pith (pith-side-coated), and no coating on both tangential surfaces (uncoated). Three adjacent quartersawn specimens were first positioned with their growth ring curvatures similarly oriented. They were then randomly assigned to three coating treatments: coating on the top radial face, coating on the bottom radial face, and no coating on both radial faces. All specimens were end-coated to minimize water evaporation from the transverse surface and to prevent end-splitting. Each set of three adjacent flatsawn or quartersawn specimens represented a replicate.

Specimens were placed in a compartment kiln and dried using the conventional moisture content-based drying schedule T4-D2 for 25- to 38-mm-thick southern red oak (Boone et al 1988). Specimens were taken out once a week and weighed to determine moisture content. Seven representative samples were also weighed everyday to monitor the drying process. The drying process was stopped after about a month when the specimens reached about 7% MC. Final moisture content of each specimen was calculated. Published shrinkage values of southern red oak from green to oven-dry condition [4.7% for radial shrinkage and 11.3% for tangential shrinkage (FPL 1999)] were used to calculate percentage shrinkage from green to final moisture content:

$$\%\mathrm{S}_{\mathrm{g-Mc}} = \frac{\%S_{g-o}(M_f - M_c)}{30} \qquad (1)$$

where $\%\mathrm{S}_{\mathrm{g-Mc}}$ = percentage shrinkage from green condition to final moisture content; $\%\mathrm{S}_{\mathrm{g-o}}$= percentage shrinkage from green to oven-dry condition; $\mathrm{M_f}$ = FSP, which was assumed to be 30%; $\mathrm{M_c}$ = final moisture content of the kiln-dried specimen.

After drying, transverse surfaces of each specimen were again scanned to model cross-sectional distortion and compare the predicted model with actual distorted shape.

Table 1. Comparison of shrinkage predicted by the model with those of actual flatsawn lumber subjected to different coating treatments (uncoated, bark-side-coated, and pith-side-coated).

					Thickness shrinkage (%)				Width shrinkage (%)				Radius of curvature for model (mm)	Radius of curvature ratio (model/actual lumber)		
Specimens[a]	R (mm)	$\theta^{(\circ)}$	Green thickness (mm)	Green width (mm)	Model	Uncoated	Bark	Pith	Model	Uncoated	Bark	Pith		Uncoated	Bark	Pith
F1A	109.92	78.71	31.10	160.69	5.44	9.23	8.07	11.21	8.12	12.53	13.07	11.48	336.93	1.79	2.95	0.25
F1B	95.53	72.82	31.44	161.20	5.70	9.34	8.82	10.07	7.78	12.56	13.23	12.83	330.37	2.11	3.44	0.47
F1C	80.59	70.97	31.53	160.95	6.20	9.40	9.95	9.31	7.56	13.62	13.82	12.58	289.71	2.67	4.33	0.64
F1D	80.45	74.10	31.44	160.95	6.26	9.68	8.82	9.80	7.67	14.37	15.67	14.66	282.90	2.60	4.08	0.72
F2A	162.20	35.30	33.37	337.34	6.59	7.37	14.47	11.58	7.96	10.52	10.81	8.79	331.36	1.56	4.61	0.58
F2B	176.36	109.39	31.83	338.03	6.20	9.81	8.40	9.77	7.81	9.88	10.18	10.20	340.99	0.91	2.58	−0.83
F2C	204.75	27.35	32.08	332.16	5.89	11.20	12.89	11.93	8.17	9.15	11.34	9.12	330.53	1.10	7.37	−0.79
F2D	178.38	35.86	31.93	332.77	5.85	10.48	10.87	12.76	7.91	9.95	12.32	10.00	388.00	1.99	6.78	−2.14
F3A	134.69	78.97	29.24	168.05	5.17	5.03	6.20	6.61	8.21	9.61	10.50	10.87	422.13	0.70	3.54	−1.50
F3B	172.32	82.28	29.32	166.54	4.70	5.68	5.93	5.93	8.48	10.44	10.96	10.96	515.34	0.79	3.80	3.80
F3C	179.63	79.04	29.51	167.12	4.61	5.44	6.72	6.39	8.41	11.41	12.01	12.18	633.33	1.30	3.41	−2.48
F3D	207.81	83.84	29.41	168.15	4.38	6.29	7.41	9.28	8.53	12.39	15.54	14.67	669.46	1.21	8.28	−1.94
F4A	75.15	75.37	30.28	169.51	6.70	8.11	9.39	9.86	7.59	11.54	12.80	12.24	281.66	2.35	2.83	0.58
F4B	71.31	79.38	29.67	166.90	6.75	8.80	8.89	9.23	7.48	12.15	13.22	11.90	271.01	2.69	3.81	1.03
F4C	62.74	77.60	29.66	166.36	6.93	9.32	9.80	9.04	7.20	11.35	12.91	11.00	262.16	2.81	4.14	0.69
F4D	150.30	43.24	29.58	167.65	6.14	8.61	8.91	7.73	7.68	11.89	14.57	11.94	287.94	2.74	4.62	1.63
F5A	81.39	100.26	29.66	160.00	6.13	9.14	10.47	8.88	7.61	11.78	11.04	12.66	292.94	1.47	3.31	−0.24
F5B	88.33	104.73	29.41	160.61	6.01	8.87	8.87	8.46	7.76	12.01	13.76	12.09	309.14	1.51	3.26	0.54
F5C	102.31	102.63	29.33	160.95	5.64	8.68	8.24	8.51	8.05	12.75	15.22	13.65	318.58	1.70	3.71	0.36
F5D	113.65	90.64	29.58	160.00	5.36	11.18	11.31	9.88	8.31	14.77	15.04	13.88	368.95	3.05	3.30	0.93
Average					5.76	8.25	8.75	8.93	7.91	11.73	12.90	11.89	363.17	1.85	4.21	0.12
Standard error					0.04	0.09	0.08	0.08	0.02	0.08	0.09	0.08	5.75	0.04	0.08	0.07

[a] Specimen designation F means flatsawn. Specimens with a common number came from the same piece of original lumber.

Numerical Determination of Pith and Shape of Original Lumber

Before modeling, two assumptions were made: 1) growth rings are arcs of perfect circles sharing the same circle center (pith of the log); and 2) shrinkage occurs tangentially along the rings and radially perpendicular to the rings (Booker et al 1992). Therefore, to predict wood distortion, finding the position of the pith or the circle center is very important. The method used here was a modification of the method used by Booker (1987). Using image analysis software Image-Pro Plus (Media Cybernetics, Inc., Bethesda, MD), coordinates of the centroid of the transverse surface of lumber were first located by connecting the four corners of the lumber cross-section. Then a curve was fitted to the growth ring arc closest to the centroid, and coordinates (x, y) of the center of the circle to which the arc belonged were obtained. Location of the circle center can be regarded as the log pith position. Distance from pith to centroid (Rc) and the angle between the bottom edge of the lumber and line PC (θc) were calculated based on coordinates (Fig 1a).

Coordinates of the four corners of the rectangular cross-section were also given by the program. Then, a spreadsheet was used to calculate coordinates of 20 equidistant points along the top edge, 20 points along the bottom edge, 5 points along the left edge, and 5 points along the right edge of the rectangle. Coordinates were originally in the Cartesian coordinate system (x, y). Coordinates of points were adjusted with the pith set as the origin. The program was previously calibrated; therefore, coordinate values were in actual lumber scale.

Modeling Lumber Cross-Sectional Distortion After Drying

Few studies have been done on numerical modeling to actually understand how cupping happens. Booker et al (1992) developed a theory using polar coordinates to describe cupping in terms of growth ring radius of curvature, growth

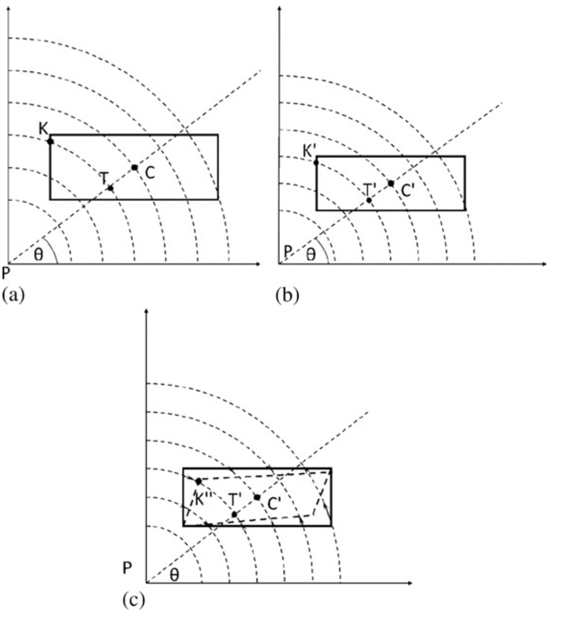

Figure 1. (a) Cross-section of lumber before shrinkage; (b) cross-section after isotropic shrinkage; (c) cross-section after further pure tangential shrinkage.

ring orientation, and stepwise radial shrinkage followed by tangential shrinkage along the growth rings. Booker (2003) later modified his model by describing cross-sectional shrinkage as an isotropic shrinkage in all directions followed by a tangential shrinkage along the growth rings. The modeling method used in this study was a modification of those described by Booker et al (1992) and Booker (2003). First, lumber was assumed to shrink isotropically from all directions by a value equal to fractional radial shrinkage (Fig 1b). Second, lumber was assumed to shrink tangentially along the growth rings toward line PC by a value equal to fractional tangential shrinkage, excluding the portion attributed previously to isotropic shrinkage (Fig 1c).

In the first step, after isotropic shrinkage in all directions, coordinates of the points on lumber became (x′, y′):

$$x' = x(1 - r) \tag{2}$$

$$y' = y(1 - r) \tag{3}$$

where r = fractional radial shrinkage from green condition to final moisture content of kiln-dried specimen. The new Cartesian coordinates x′, y′ were transformed to polar coordinates (R, θ):

$$R = \sqrt{x'^2 + y'^2} \qquad (4)$$

$$\theta = \arctan\frac{y'}{x'} \qquad (5)$$

In the second step, lumber underwent pure tangential shrinkage by an amount equal to (1 − t)/(1 − r) along the growth rings toward line PC, because the portion that shrank in the first step had to be excluded to maintain a total tangential shrinkage of t. Thus, arc KT became arc K′T′ after isotropic radial shrinkage and subsequently became arc K″T″ after tangential shrinkage:

$$K'T' = KT \times (1 - r) \qquad (6)$$

$$K''T'' = KT \times (1 - t) \qquad (7)$$

Thus,

$$K''T'' = K'T' \times \frac{(1 - t)}{(1 - r)} \qquad (8)$$

where r was as defined previously and t = fractional tangential shrinkage from green condition to final moisture content of the kiln-dried specimen.

Therefore, each point on K′T′ changed from coordinates (R, θ) to (R, θ′) on K″T″, and the angle changed from θ_a to $\theta_{a'}$:

$$R \cdot \theta a' = (R \cdot \theta a) \times \frac{(1 - t)}{(1 - r)} \qquad (9)$$

$$\theta' - \theta c = (\theta - \theta c) \times \frac{(1 - t)}{(1 - r)} \qquad (10)$$

$$\theta' = (\theta - \theta c) \times \frac{(1 - t)}{(1 - r)} + \theta c \qquad (11)$$

where θ_a and $\theta_{a'}$ = angles occupied by arc K′T′ and K″T″, respectively; and θ_c = angle between bottom edge of lumber and line PC (Fig 1).

The new polar coordinates (R, θ′) were changed back to Cartesian coordinates (x″, y″), where x″ = R·cos(θ′) and y″ = R·sin(θ′). The new coordinates were again graphed using a spreadsheet and compared with original lumber and the real distorted shape of the lumber.

In Booker's method (Booker 2003), after isotropic shrinkage in all directions, lumber underwent a pure tangential shrinkage by a value of (1 − t + r) instead of (1 − t)/(1 − r). Therefore, total tangential shrinkage along growth rings was underestimated.

Experimental Verification

To verify the model, simple visual comparison with actual lumber is not sufficient. Numerical differences between the model and the actual sample need to be shown to determine how well the predicted model agrees with the real cross-sectional distortion.

For flatsawn lumber, width and thickness of the predicted model or deformed lumber were determined based on distances between the four corners of the lumber. For example, distance from the top left to top right corners gave the top width, whereas distance from the bottom left to bottom right corners gave the bottom width. Left side and right side thickness were obtained similarly. Top and bottom width were averaged and then compared with average width of green lumber to obtain percentage shrinkage in width. The same calculations were performed to obtain percentage shrinkage in thickness. Radii of curvature for the two wide lumber faces were also measured and averaged. If lumber cupped toward the tangential surface close to the pith, radius of curvature for that lumber was defined as negative. The ratio of radius of curvature for the model to radius of curvature for the actual lumber was calculated. A ratio of 1 meant that the model and actual lumber had the same degree of cupping. If the ratio was greater than 1, it meant that the actual lumber had more cupping than the model; conversely, if it was less than 1, the actual lumber had less cupping than the model. If the value was negative, it meant that the actual lumber had cupping toward the opposite side.

For quartersawn lumber, only width and thickness shrinkage for the predicted model and the actual sample were measured.

RESULTS AND DISCUSSION

Model Verification of Lumber Cross-Sectional Distortion After Drying

To verify how close the predicted model was to the actual lumber cross-section, uncoated specimens were compared. For flatsawn lumber, average thickness shrinkage was 5.76 ± 0.04% for the predicted model and 8.30 ± 0.09% for uncoated specimens. Average width shrinkage was 7.91 ± 0.02% for the predicted model and 11.73 ± 0.08% for uncoated specimens. The ratio of radii of curvature was 1.85 ± 0.04 (Table 1). For quartersawn lumbers, average thickness shrinkage was 7.38 ± 0.23% for the predicted model and 14.03 ± 0.74% for uncoated specimens. Average width shrinkage was 4.94 ± 0.24% for the predicted model and 7.33 ± 0.41% for uncoated specimens (Table 2).

Predicted shapes of lumber cross-sections were in close agreement with those of actual specimens (Fig 2). Booker et al (1992) found closer agreement between his model and experimental results. However, in that study, a different lumber species, radiata pine, was evaluated, which has much less radial shrinkage (1.61%) and tangential shrinkage (3.69%) than the species used in this study (southern red oak). Southern red oak has radial and tangential shrinkage values from green to oven-dry of 4.7 and 11.3%, respectively.

In this study, the model agreed better with actual distortion for flatsawn lumber groups F2, F3, and F5 and less with flatsawn lumber groups F1 and F4, which indicated that there were percentage shrinkage variations among lumber from

Table 2. Comparison of shrinkage of predicted model with those of quartersawn lumber subjected to different coating treatments (uncoated, bark-side-coated, and pith-side-coated).

					Thickness shrinkage (%)				Width shrinkage (%)			
Specimens[a]	R (mm)	$\theta^{(\circ)}$	Green thickness (mm)	Green width (mm)	Model	Uncoated	Upper-coated	Bottom-coated	Model	Uncoated	Upper-coated	Bottom-coated
Q1A	137.42	−1.55	29.24	139.41	8.82	13.89	16.85	15.09	3.76	6.20	6.26	6.69
Q1B	374.18	−7.25	30.01	142.12	8.80	16.92	15.82	15.92	3.78	5.31	5.55	6.42
Q1C	282.77	−12.15	30.43	141.21	8.39	18.38	17.59	16.50	3.89	5.29	5.19	6.06
Q1D	60.49	−2.65	30.09	138.52	7.84	17.19	16.98	17.80	3.59	5.17	5.51	5.65
Q2A	89.90	9.60	28.99	137.04	7.96	16.24	14.58	14.96	4.06	5.73	5.38	4.54
Q2B	147.58	13.96	28.90	141.61	8.35	16.53	18.10	18.55	4.12	6.58	7.33	6.51
Q2C	121.00	16.35	29.07	143.90	7.86	17.19	15.65	17.78	4.28	4.67	6.72	6.22
Q2D	127.77	16.18	29.16	145.59	7.95	17.64	15.95	15.99	4.28	5.99	6.67	6.21
Q3A	390.30	12.17	31.02	148.75	8.52	18.49	19.21	21.39	3.87	5.79	6.39	5.52
Q3B	537.52	22.33	32.38	147.30	7.99	17.73	17.42	15.27	4.35	6.50	6.09	6.90
Q3C	579.79	23.48	31.44	144.94	7.99	16.27	15.47	13.59	4.40	6.50	7.25	7.35
Q3D	235.01	20.94	30.26	144.17	7.92	13.66	14.69	14.69	4.28	5.98	7.29	7.62
Q4A	275.18	28.67	29.41	154.84	7.37	10.02	14.85	31.92	4.96	8.21	7.50	7.81
Q4B	149.37	36.60	29.75	155.00	6.40	10.75	11.73	15.00	5.75	8.86	9.59	9.25
Q4C	164.26	39.39	29.75	154.50	6.33	13.42	9.65	7.75	5.94	9.10	9.43	10.18
Q4D	70.12	39.65	29.16	154.07	6.60	11.65	15.89	12.49	6.26	9.29	10.15	10.01
Q5A	225.11	40.92	31.95	226.95	6.04	7.97	17.37	15.61	6.12	9.24	9.01	8.06
Q5B	175.79	51.79	30.69	231.72	5.50	9.36	10.80	8.01	7.01	10.83	11.30	13.66
Q5C	212.64	55.59	30.89	227.98	5.23	8.34	10.38	7.90	7.29	10.83	11.94	11.97
Q5D	369.98	51.11	30.02	225.61	5.64	9.00	7.64	7.63	6.83	10.50	10.74	12.69
Average					7.38	14.03	14.83	15.19	4.94	7.33	7.76	7.97
Standard Error					0.23	0.74	0.63	1.10	0.24	0.41	0.42	0.51

[a] Specimen designation Q means quartersawn. Specimens with a common number came from the same piece of original lumber.

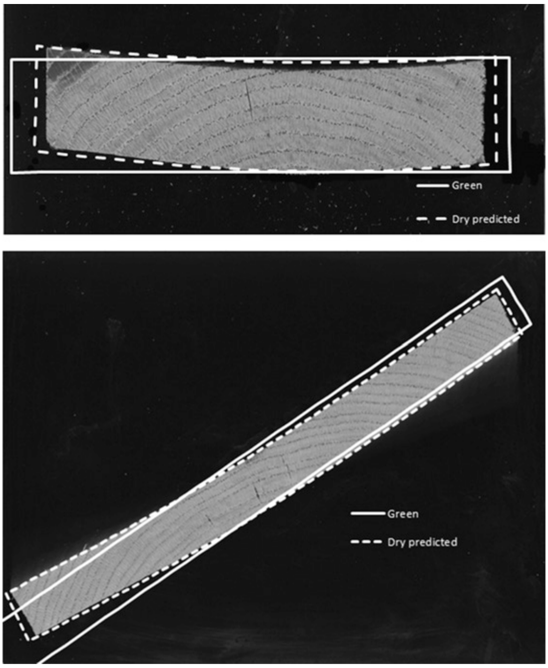

Figure 2. Comparison of predicted cross-sectional lumber distortion (dashed outline) with actual lumber distortion (photograph) after drying. Also shown are green lumber shapes (solid outline).

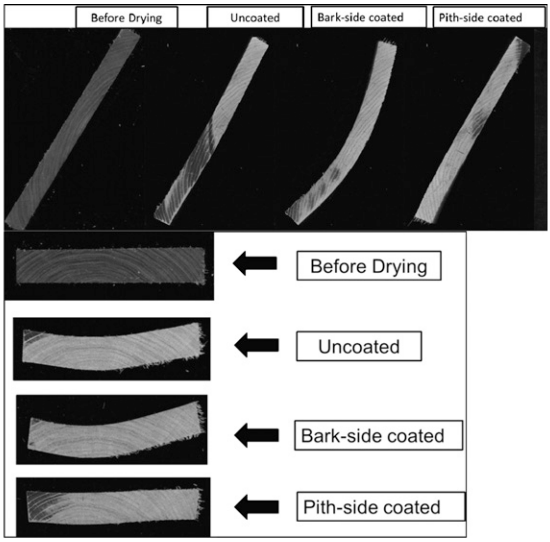

Figure 3. For flatsawn lumber, bark-side-coated specimens had more severe cupping and pith-side-coated specimens had less cupping (even cupping toward the opposite side compared with uncoated specimens).

different trees. Also, width shrinkage (7.33%) and thickness shrinkage (14.03%) of quartersawn lumber in this study were much greater than radial and tangential percentage shrinkage values from the literature (FPL 1999). This is a possible source of error because the literature values were used in modeling cross-sectional distortion. Instead of taking shrinkage values from the literature, Booker et al (1992) measured actual percentage shrinkage values for their specimens and thus observed less difference in distortion between the model and actual lumber.

Effects of Drying Stresses on Lumber Distortion After Drying

All coated flatsawn lumber had similar thickness shrinkage of about 8.5% but had significantly different width shrinkage, ranging from 11.7-12.9%. Bark-side-coated specimens had a radius of curvature ratio of about 4.2, which was much larger than the 1.9 ratio for uncoated specimens. This indicates that bark-side-coated specimens had very severe cupping. Pith-side-coated specimens had a radius of curvature ratio of about 0.1, which was much smaller than that of uncoated specimens, indicating little or no cupping (Table 1). Several pith-side-coated specimens even cupped toward the opposite side (Fig 3). For quartersawn lumber, no evident cupping and no significant difference among the differently treated specimens occurred (Fig 4).

The fact that flatsawn lumber had such response to coating treatment could be explained by drying stress imbalance. For uncoated specimens, at the initial stage of drying, the lumber surface dries first and starts to shrink, whereas the lumber core is still wet and does not shrink. This causes the lumber surface to be in tension stress and the core in compression stress (Fig 5a). However, stresses are balanced within the lumber, therefore the lumber has normal cupping mainly caused by greater shrinkage of the face near the bark relative to that of the face near the pith. For pith-side-coated specimens, tension stress is closer to the bark side and compression

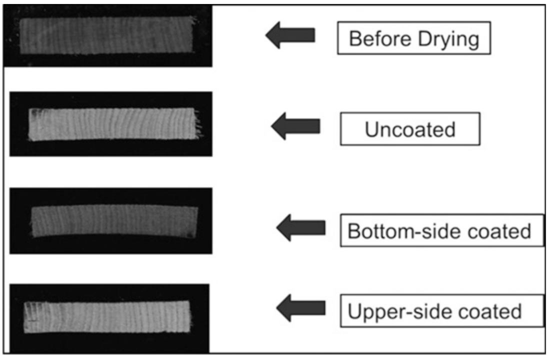

Figure 4. Quartersawn specimens showing no evident cupping and no significant difference among differently treated specimens.

stress is closer to the pith side at the initial stage of drying (Fig 5b). If the portion in tension exceeds the tensile stress at proportional limit perpendicular to the grain, it assumes a tensile set and is therefore in an expanded state. Similarly, if the portion in compression exceeds the compressive stress at proportional limit perpendicular to the grain, it assumes a compressive set and is therefore in a contracted state. Shrinkage of the face near the bark is offset by the tensile set whereas shrinkage of the face near the pith is in the same direction as the compressive set and, therefore, lumber has less cupping when coated on the pith side. In fact, if the tensile set is larger than the shrinkage of the face near the bark and/or the compressive set is larger than the shrinkage of the face near the pith, the lumber could cup toward the opposite side (Fig 3). For bark-side-coated lumber, stress distribution is the reverse of the pith-side-coated specimens (Fig 5c). Lesser shrinkage of the face near the pith (relative to that of the face near the bark) is exacerbated by the tensile set on that face and by the compressive set on the other face, thereby resulting in more severe cupping.

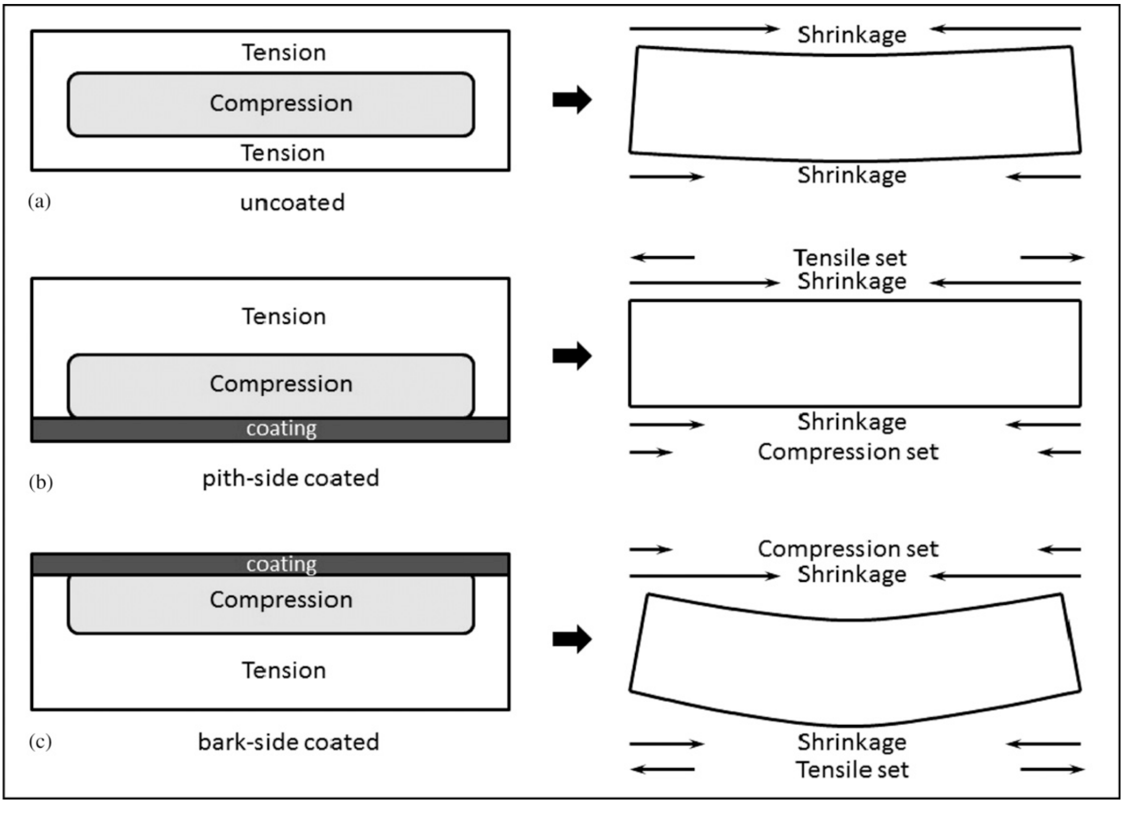

Figure 5. Drying stress analysis of (a) uncoated, (b) pith-side-coated, and (c) bark-side-coated specimens.

The decreased amount of cupping in pith-side-coated specimens suggests that simple application of surface coating on lumber prior to drying could potentially minimize the amount of warp during drying. This concept must be explored further because the approach is very simple and the cost associated with its implementation appears minimal.

CONCLUSIONS

In this study, southern red oak lumber cross-sectional shrinkage after drying was analyzed. The predicted shape of the lumber cross-section after drying was compared with actual lumber distortion. The predicted model closely agreed with actual distortion with the difference mainly attributed to use of published shrinkage values instead of measuring actual percentage shrinkages.

Bark-side-coated lumber had more cupping and pith-side-coated lumber had less cupping compared with uncoated specimens. The reason for this was unbalanced drying stress. To better model drying distortion of bark-side-coated and pith-side-coated specimens, drying stresses need to be incorporated. This could be the subject of a future study. Surface-coating lumber close to the pith could be a novel approach to minimizing lumber warp during drying.

ACKNOWLEDGMENTS

This project was supported by the National Research Initiative of the USDA-CSREES, grant number 2005-35504-16145.

REFERENCES

Booker R (2003) Shrinkage and theories of differential shrinkage. Pages 29-45 *in* Wood Research, EMPA-Symposium, 17 January 2003, Eidgenössische Materialprüfungs- und Forschungsanstalt, Dubendorf, Switzerland.

Booker R, Ward N, Williams Q (1992) A theory of cross-sectional shrinkage distortion and its experimental verification. Wood Sci Technol 26(5):353-368.

Booker RE (1987) A method for recording annual ring orientation in boards. Forest Prod J 37(6):31-33.

Boone RS, Kozlik CJ, Bois PJ, Wengert EM (1988) Dry kiln schedules for commercial woods—Temperate and tropical. Gen Tech Rep FPL-GTR-57 USDA For Serv Forest Prod Lab, Madison, WI. 158 pp.

Ferguson WJ (1997) A numerical prediction of the effect of airflow and wet bulb temperature on the stress development during convective wood drying. Pages 260-269 *in* I Turner and AS Mujumdar, eds. Mathematical modeling and numerical techniques in drying technology. Marcel Dekker, Inc., New York, NY.

FPL (2001) Dry kiln operator's manual. USDA For Serv Forest Prod Lab, Madison, WI. 274 pp.

FPL (1999) Wood handbook: Wood as an engineering material. Gen Tech Rep FPL-GTR-113. USDA For Serv Forest Prod Lab, Madison, WI. 463 pp.